Thermal phase transition of generalized Heisenberg models for SU(N) spins on square and honeycomb lattices

Suzuki, Takafumi; Harada, Kenji; Matsuo, Haruhiko; Todo, Synge; Kawashima, Naoki

PHYSICAL REVIEW B **91**, 094414 (2015)

Thermal phase transition of generalized Heisenberg models for SU(N) spins on square and honeycomb lattices

Takafumi Suzuki,[1] Kenji Harada,[2] Haruhiko Matsuo,[3] Synge Todo,[4] and Naoki Kawashima[5]
[1]*Graduate School of Engineering, University of Hyogo, Hyogo, Himeji 670-2280, Japan*
[2]*Graduate School of Informatics, Kyoto University, Kyoto 615-8063, Japan*
[3]*Research Organization for Information Science and Technology, Kobe 650-0047, Japan*
[4]*Department of Physics, University of Tokyo, Tokyo 113-0033, Japan*
[5]*Institute for Solid State Physics, University of Tokyo, Kashiwa 277-8581, Japan*
(Received 1 October 2014; revised manuscript received 20 February 2015; published 16 March 2015)

We investigate thermal phase transitions to a valence-bond solid phase in SU(N) Heisenberg models with four- or six-body interactions on a square or honeycomb lattice, respectively. In both cases, a thermal phase transition occurs that is accompanied by rotational symmetry breaking of the lattice. We perform quantum Monte Carlo calculations in order to clarify the critical properties of the models. The estimated critical exponents indicate that the universality classes of the square- and honeycomb-lattice cases are identical to those of the classical XY model with a Z_4 symmetry-breaking field and the three-state Potts model, respectively. In the square-lattice case, the thermal exponent, ν, monotonically increases as the system approaches the quantum critical point, while the values of the critical exponents, η and γ/ν, remain constant. From a finite-size scaling analysis, we find that the system exhibits weak universality, because the Z_4 symmetry-breaking field is always marginal. In contrast, ν in the honeycomb-lattice case exhibits a constant value, even in the vicinity of the quantum critical point, because the Z_3 field remains relevant in the SU(3) and SU(4) cases.

DOI: 10.1103/PhysRevB.91.094414 PACS number(s): 05.10.Ln, 75.10.Jm, 75.40.Cx, 75.40.Mg

I. INTRODUCTION

The classification of various continuous phase transitions has been successfully discussed from the viewpoint of the Landau-Ginzburg-Wilson (LGW) paradigm [1,2]. The essential principles of the paradigm are the clarification of (local) order parameters and the characterization of breaking symmetries. Recently, the possibility of deconfined critical phenomena (DCP) [3–5] has attracted considerable attention as a quantum phase transition (QPT) beyond the LGW paradigm. DCP have been predicted to occur at the QPT point between a magnetically ordered phase, such as the Néel phase, and the valence-bond solid (VBS) phase in two dimensional (2D) systems. Remarkably, this phase transition is continuous, although the symmetry group in one phase is not the subset of another phase. The well-known models that are expected to exhibit DCP are the generalized Heisenberg models with multibody interactions for SU(N) spins, namely, SU(N) JQ_m models [6]. Considerable effort has been expended to numerically determine whether the QPT of this model family is of the second order or weak first order; however, a satisfactory result has not yet been obtained [6–14].

An interesting aspect of DCP is that the transition may occur independently of the lattice geometry [4,5]. In a previous study [14], we evaluated the critical exponent, $\nu_{\rm QPT}$, at the QPT point between the Néel and VBS phase in SU(N) JQ_m models on both square and honeycomb lattices using quantum Monte Carlo (QMC) calculations. From the finite-size scaling (FSS) analysis, we confirmed that $\nu_{\rm QPT}$ is independent of the lattice geometry but depends on the SU(N) symmetry. This result strongly suggested the presence of DCP in the SU(N) JQ_m models. However, $\nu_{\rm QPT}$ for the SU(3) models exhibits a systematic shift toward the trivial value of $\nu_{\rm QPT} = 1/D (D = 3)$ as the system size increases. Therefore, the possibility of a first-order transition remains in the case of SU(3).

The nature of the QPT point is important in the discussion of finite-temperature properties, because it can strongly affect the topology of the thermal phase diagram and also the criticality, as shown in Fig. 1. The SU(N) JQ_m models are expected to exhibit a thermal phase transition if the VBS pattern is characterized by spontaneous symmetry breaking of the lattice. Thus, consideration of the critical properties of thermal transitions in the vicinity of the QPT point may yield a different perspective on the possibility of DCP occurring in SU(N) JQ_m models.

The universality class of the thermal transition has been discussed for both SU(2) JQ_2 [15] and JQ_3 [16] models on the square lattice. The VBS pattern on the square lattice is described by a columnar dimer configuration, which is characterized by the spontaneous breaking of $\pi/2$ rotational symmetry around the center of the plaquette. Thus, the Z_4 symmetry breaking of the VBS order parameter is expected at the critical temperature. In the 2D case, several models that exhibit Z_4 symmetry breaking exist, such as the Ashkin-Teller model [17] including the four-state Potts model [18] and the 2D classical XY spin model with the Z_4 field ($XY + Z_4$ model). In such models, the critical exponent, η, always satisfies the condition $\eta = 1/4$. However, the observed exponent $\eta \sim 0.59$ of the SU(2) JQ_2 model differs from the expected value [15]. In the SU(2) JQ_2 model, the VBS order is very weak because the QPT point is located in the vicinity of the limit, and the model can only be expressed using the multibody interacting Q_m term (the dimer limit). To enhance the VBS order, Jin and Sandvik have focused on the SU(2) JQ_3 models [16]. The QMC results they have obtained [16] indicate that the criticality is well explained by the Gaussian conformal-field theory with central charge $c = 1$; the thermal exponent, ν, monotonically increases as the system approaches the QPT point, while the following relations between the exponents, $\eta = 1/4$, $\gamma/\nu = 7/4$, and $\beta/\nu = 1/8$, are retained. This is

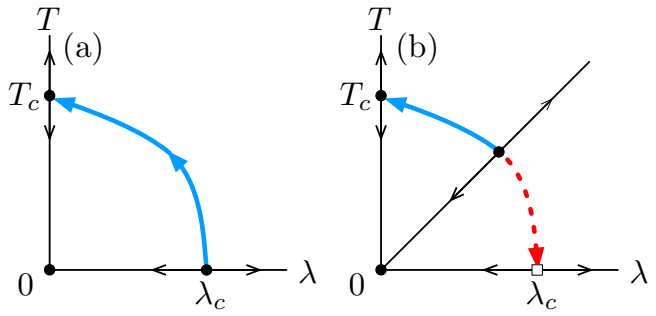

FIG. 1. (Color online) Schematic phase diagram and renormalization flow. The thick solid (dashed) curves correspond to the second (first)-order transition. The horizontal axis, λ, is the coupling ratio of the Heisenberg term J and the multibody interaction term Q_m. The open square represents a discontinuous transition. Each solid circle denotes a fixed point, such as the 2D Ising, three-state Potts, and multicritical fixed points. The coordination origin corresponds to the low-temperature fixed point. All arrows indicate renormalization flows. (a) DCP scenario. (b) First-order transition scenario.

a characteristic aspect of the 2D weak Ising universality class [19], and the same behavior has also been observed in the 2D $XY + Z_4$model [20–22]. In the case of the classical spin model, ν monotonically increases as the Z_4 symmetry-breaking field, h_4, is suppressed and finally diverges at the XY limit, where the Kosterliz-Thouless (KT) transition takes place. Jin and Sandvik [16] have observed that an enhancement of the U(1) symmetry of the VBS order parameter is observed at close proximity to the transition temperature and the QPT point, when the system size is smaller than a characteristic length scale. Since it has been noted that the emergence of additional U(1) symmetry is an important signature of DCP [5,9], the numerical result in Ref. [16] is consistent with the presence of a deconfined critical point in the SU(2) JQ_3 model. However, the observation of U(1) symmetry in the vicinity of the QPT point seems to be natural, because the Z_4 field in the classical model is always marginal at a transition temperature and the system becomes the pure XY model at the $h_4 \to 0$ limit [20]. Thus, the emergence of U(1) symmetry cannot be regarded as sufficient evidence for the presence of a deconfined critical point in this case. Since the possibility of a first-order transition has been suggested in the SU(3) JQ_2 model case [14], where the same Z_4 field is broken, systematic studies of SU(N) symmetry are necessary.

In contrast to the square-lattice case, the nature of the symmetry-breaking field is different for the honeycomb-lattice case. When the columnar VBS pattern is characterized by $\pi/3$ rotational symmetry breaking, the corresponding classical model is expected to be the $XY + Z_3$ model. Since the Z_3 field is relevant in two dimensions, the universality class is explained by the 2D three-state Potts model [23], and the emergence of the U(1) symmetry in the VBS order parameter may then be suppressed in the vicinity of the QPT. Although this is correct in the case of SU(2) spins, the higher SU(N)-symmetric case seems to be controversial. The discussion of DCP is based on the noncompact complex projective (NCCP^{N-1}) theory with Z_k symmetry-breaking fields [3,5]. In this theory, although the Z_3 symmetry-breaking field is relevant, it becomes irrelevant as N increases [4,24]. For the SU(2) case, which corresponds to the NCCP[1] theory, recent QMC results have indicated that the Z_3 field is *relevant* but almost marginal at the QPT [13]. Therefore, one can expect the first-order transition at the QPT point in the SU(2) case and a change of criticality as N increases. This indicates that the criticality of the thermal transitions and the topology of the phase diagram are determined based on the order of the QPT. If the QPT is continuous, as is expected for larger values of N, and the system approaches the QPT, whether or not the universality classes of the thermal transition are affected is a nontrivial question.

Our previous QMC calculations suggest that the same criticality exists at the QPT regardless of the lattice geometry [14]. This implies that the phase diagram topologies are identical in both the square- and the honeycomb-lattice cases. If one focuses on the most likely and simplest case, two scenarios for the thermal phase diagram can be expected depending on the order of the QPT point: (a) the QPT transition is of the second order and the thermal transition is always continuous [Fig. 1(a)], and (b) the QPT is a weak first-order transition and the multicritical point exists at a finite temperature [Fig. 1(b)]. When scenario (b) occurs, we expect to observe crossover behavior and for ν to change to the trivial value, $\nu = 1/D$ ($D = 2$). From the above discussion, the importance of calculating the thermal phase diagram for different values of N and various lattice geometries with high accuracy is apparent. Further, such calculations can allow us to consider the possibility of the DCP scenario in the SU(N) JQ_m models. Thus, in this paper, we systematically study the thermal phase transitions of the JQ_2 model on the square lattice and the JQ_3 model on the honeycomb lattice for SU(3) and SU(4) spins.

The layout of this paper is as follows. In Sec. II, we study the thermal transition of the SU(N) JQ_m model. We begin by introducing the model details and the order parameters evaluated in the QMC computations. In Sec. III, we present the results of the finite-size scaling analysis for the obtained numerical data. The criticality of the thermal transition is discussed for the square-lattice and the honeycomb-lattice cases. Then, we discuss possible scenarios for the QPT of both models from the perspective of the thermal phase diagram. Finally, we summarize our results in Sec. IV.

II. MODEL AND METHOD

We consider the SU(N) JQ_2 model on the square lattice and the SU(N) JQ_3 model on the honeycomb lattice. Both models are simply expressed by the color-singlet-projection operator, P_{ij}, which is defined as $P_{ij} = -\frac{1}{N}\sum_{\alpha=1}^{N}\sum_{\beta=1}^{N} S_i^{\alpha\beta}\bar{S}_j^{\beta\alpha}$, where $S_i^{\alpha\beta}$ is the SU(N) spin generator and $\bar{S}_j^{\beta\alpha}$ is its conjugate. The model Hamiltonian can be expressed as

$$\mathcal{H} = -J\sum_{(ij)} P_{ij} - Q_2 \sum_{(ij)(kl)} P_{ij}P_{kl}, \tag{1}$$

for the square-lattice case, and

$$\mathcal{H} = -J\sum_{(ij)} P_{ij} - Q_3 \sum_{(ij)(kl)(mn)} P_{ij}P_{kl}P_{mn}, \tag{2}$$

for the honeycomb-lattice case, where (ij) indicates the nearest-neighbor sites. The summation for the Q_m terms runs

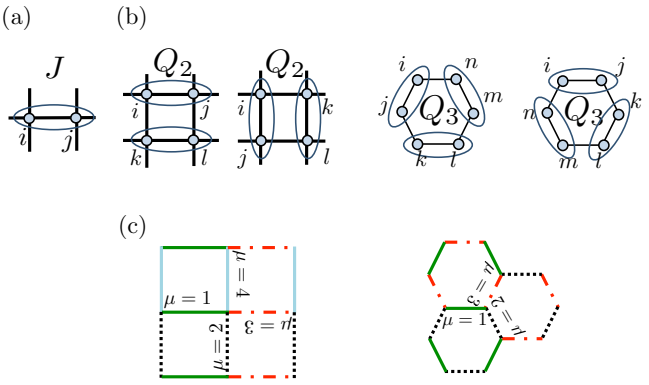

FIG. 2. (Color online) (a) Color-singlet projection operator on a bond. The bold ellipsoids denote a color-singlet dimer state and correspond to P_{ij}'s. (b) Projection operators for Q_2 and Q_3 terms. (c) Coordination index, μ.

over all pairs without breaking the rotational symmetry of the lattice, as illustrated in Fig. 2. Since the present lattices are bipartite, the fundamental (conjugate) representation is adapted for the SU(N) spins on A(B) sites.

For Hamiltonians (1) and (2), we performed QMC calculations up to $L = 256$ for the square-lattice case and $L = 132$ for the honeycomb-lattice case, respectively. (The number of sites, $\mathcal{N}$, corresponds to $\mathcal{N} = L^2$ and $\mathcal{N} = 2L^2$, respectively.) The QMC code used here is based on the massively parallelized loop algorithm [25] provided in the ALPS project code [26]. In the computations, we measured the VBS amplitude, which is defined as $\Psi_{\boldsymbol{r}} \equiv \sum_{\mu=1}^{z} \exp[\frac{2\pi i}{z}\mu]\hat{P}_{\boldsymbol{r},\boldsymbol{r}_\mu}$, where $\hat{P}_{\boldsymbol{r},\boldsymbol{r}_\mu}$ is the diagonal component of the projection operator, z is the coordination number of a lattice, and $\boldsymbol{r}_\mu$ represents the neighboring site of $\boldsymbol{r}$ in the μ direction [see Fig. 2 (b)]. From $\Psi_{\boldsymbol{r}}$, the VBS order parameter, which is defined as $\Psi \equiv L^{-2}\sum_{\boldsymbol{r}} \Psi_{\boldsymbol{r}}$. After $\Psi_{\boldsymbol{r}}$ was evaluated, we obtained further quantities: the Binder ratio, $B_R \equiv \langle\Psi^4\rangle/\langle\Psi^2\rangle^2$; the VBS correlation function, $C(\boldsymbol{r}) \equiv \langle\Psi_{\boldsymbol{r}}\Psi_{\boldsymbol{0}}\rangle$; the correlation ratio, $C_R \equiv \frac{C(L/2,L/2)}{C(L/4,L/4)}$; the correlation length, $\xi \equiv \frac{1}{|\Delta\boldsymbol{Q}|}\sqrt{\frac{S(\boldsymbol{Q}_c)}{S(\Delta\boldsymbol{Q})} - 1}$; and the static structure factor, $S(\boldsymbol{Q}) = L^{-2}\sum_{\boldsymbol{r},\boldsymbol{r}'} \exp[-i\,\boldsymbol{Q}(\boldsymbol{r} - \boldsymbol{r}')]\langle\Psi_{\boldsymbol{r}}\Psi_{\boldsymbol{r}'}\rangle$. Here, $\Delta\boldsymbol{Q}$ denotes the distance between the order wave-vector, $\boldsymbol{Q}_c = \boldsymbol{0}$, and the nearest-neighbor positions, $(0, 2\pi/L_y)$ or $(2\pi/L_x, 0)$.

In this paper, we discuss the thermal transition criticality by changing the coupling constants, J and Q_m. It is convenient to introduce a length scale associated with the distance from the QPT point, where the ground state changes from the Néel state to the VBS state. The QPT points were previously evaluated in Ref. [14] and are summarized in Table I. The coupling ratio, $\lambda = J/(J + Q_m)$, of the QPT point depends strongly on the lattice geometry and also on the degree of freedom of the SU(N) spin. Therefore, we introduce a normalized coupling constant that is defined as $\Lambda = \lambda/\lambda_c$, where λ_c is the critical value at the QPT point. From this definition, one can easily see that $\Lambda = 0$ and 1 correspond to the dimer limit and the QPT point, respectively.

TABLE I. Critical points of SU(N) $J\,Q_m$ models. λ_c is the critical value of the coupling ratio defined as $\lambda \equiv J/(J + Q_m)$, where J and Q_m are the coupling constants. All values are given in Ref. [14].

SU(N)	$J\,Q_2$	$J\,Q_3$
2	$\lambda_c = 0.042$	$\lambda_c = 0.456$
3	$\lambda_c = 0.665$	$\lambda_c = 0.796$
4	$\lambda_c = 0.917$	$\lambda_c = 0.985$

III. NUMERICAL RESULTS AND FINITE-SIZE SCALING ANALYSIS

In Figs. 3 and 4, we show the temperature dependence of C_R, B_R, ξ, and $S(\boldsymbol{Q}_c)$ at $\Lambda = 0.5$, which is the middle distance between the QPT point and the dimer limit. Since clear crosses are always observed for $0 \leqslant \Lambda \lesssim 1$ as the temperature decreases, the thermal transition from the paramagnetic to the VBS phase is expected to be of the second order.

To discuss the universality class, we performed a FSS analysis of ξ, C_R, B_R, and $S(\boldsymbol{Q}_c)$, assuming the scaling forms $\xi/L \sim g_\xi[L^{y_t}(T - T_c)]$, $C_R \sim g_{C_R}[L^{y_t}(T - T_c)]$, $B_R \sim g_{B_R}[L^{y_t}(T - T_c)]$, and $S(\boldsymbol{Q}_c)L^{-\frac{\gamma}{\nu}} \sim g_{S_Q}[L^{y_t}(T - T_c)]$, where $y_t = \nu^{-1}$ and $g_X[x]$ is a scaling function. We applied the Bayesian scaling analysis [27] to the FSS analysis of larger system-size sets and estimated the values as follows. First, the critical temperature, T_c, and y_t were evaluated from

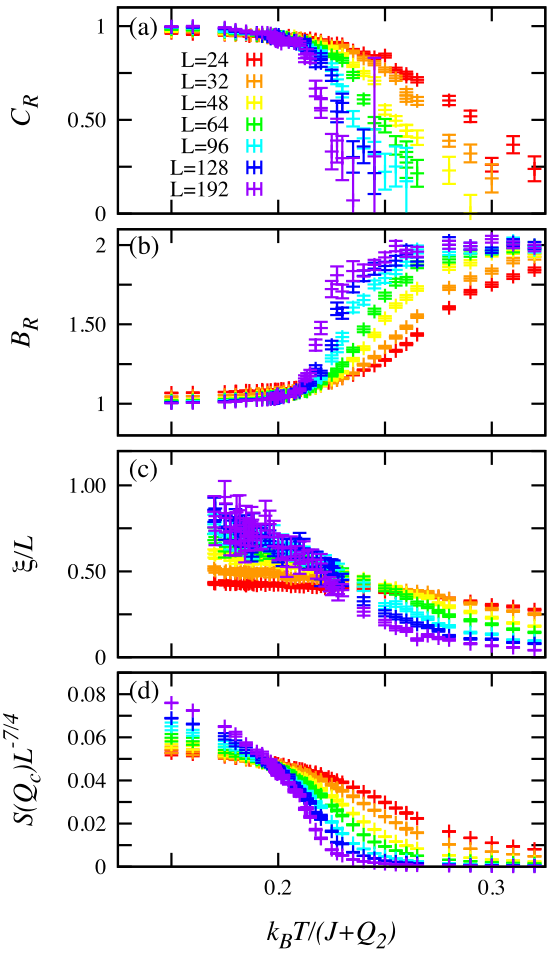

FIG. 3. (Color online) Temperature dependence of C_R, B_R, ξ/L, and $S(\boldsymbol{Q}_c)L^{-\frac{\gamma}{\nu}}$ in the SU(3) square-lattice model at $\Lambda = 0.5$.

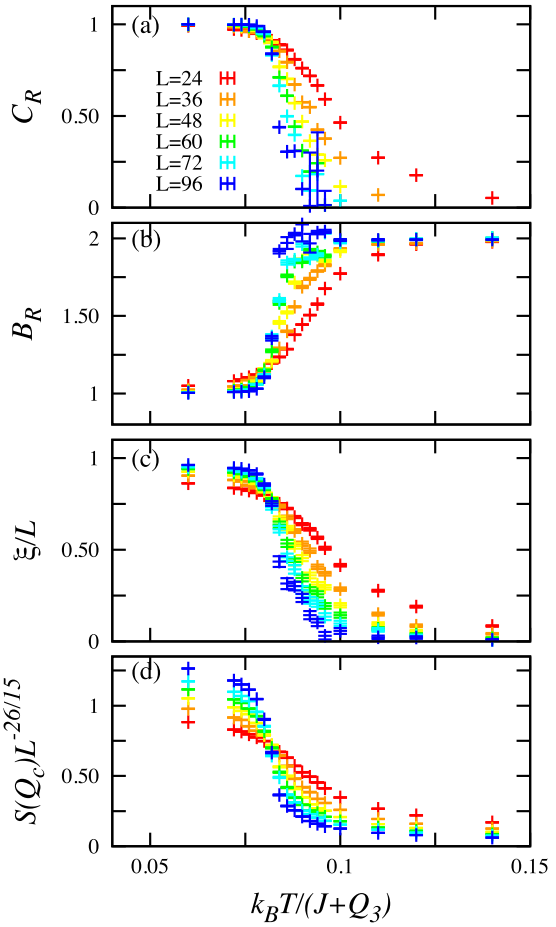

FIG. 4. (Color online) Temperature dependence of C_R, B_R, ξ/L, and $S(\boldsymbol{Q}_c)L^{-\frac{\gamma}{\nu}}$ for the SU(4) honeycomb-lattice model at $\Lambda = 0.5$.

ξ and C_R (or ξ and the Binder ratio B_R), because their scaling forms contain only two variables, T_c and y_t. Both T_c and y_t were optimized simultaneously from the ξ and C_R data set. In detail, we evaluated T_c and y_t for several data sets labeled $L_{\max}$ that include four different system sizes, for example, $L_{\max} = 72$ includes $L = \{32,48,64,72\}$, $L_{\max} = 96$ includes $L = \{48,64,72,96\}$, and so on. Since apparent system-size dependence is observed for $\Lambda > 0$, we evaluated the extrapolated values of T_c and y_t in the limit $L_{\max} \to \infty$ from the large-system sets. (One example of this size dependence is the result at $\Lambda = 0.15$ for SU(3) shown in Fig. 7.) After we obtained T_c and y_t for the thermodynamic limit, η and γ/ν were independently obtained from the correlation function, $C(\boldsymbol{r})$, and $S(\boldsymbol{Q}_c)$.

We summarize the estimated $y_t(= \nu^{-1})$ and T_c in Fig. 5 for the square-lattice case (the SU(N) JQ_2 model). In the square-lattice model, y_t (ν) monotonically decreases (increases) as the system approaches the quantum critical point, in both the SU(3) and the SU(4) cases. In contrast to y_t, we observe that η and γ/ν take constant values for $\Lambda < 0.97$. Figures 6(a) and 6(b) show the Λ dependence of the effective η estimated from the assumption that $C(R) \sim R^{-\eta}$. From Figs. 6(a) and 6(b), it is apparent that η clearly crosses $\eta = 1/4$ at critical temperatures within the error bars. In the same manner, the effective γ/ν is estimated from the form $S(\boldsymbol{Q}_c = 0) \sim L^{\gamma/\nu}$.

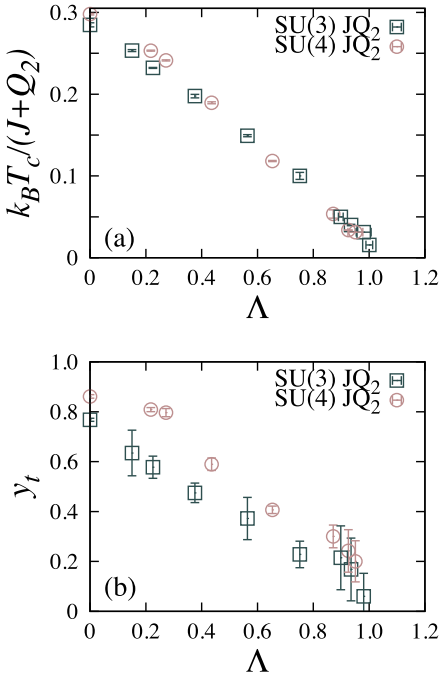

FIG. 5. (Color online) (a) Critical temperature and (b) renormalization group eigenvalue, y_t, for temperature in the square-lattice case. The open squares (circles) are the SU(3) [SU(4)] results. y_t is estimated by extrapolation to the thermodynamic limit, $\Lambda = 0$ corresponds to the dimer limit, where $J = 0$, and $\Lambda = 1$ is the QPT point.

Figures 6(c) and 6(d) present γ/ν evaluated from the data for $L \geqslant 96$. We can confirm from Fig. 6 that γ/ν crosses the value 7/4 at critical temperatures. Thus we conclude that η and γ/ν satisfy $\eta = 1/4$ and $\gamma/\nu = 7/4$ at critical temperatures, within the error bars. The obtained exponents are the same as those of

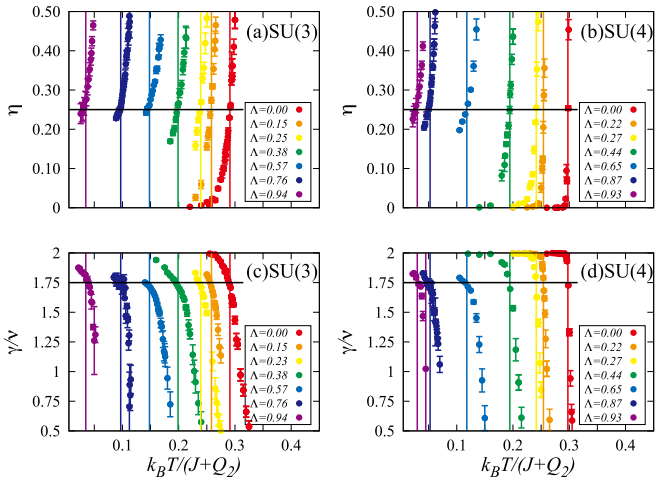

FIG. 6. (Color online) Λ dependence of effective η and γ/ν of SU(N) JQ_2 models. All values were evaluated from the assumptions $C(R = L/\sqrt{2})|_{T\sim T_c} \sim L^{-\eta}$ and $S(\boldsymbol{Q}_c)|_{T\sim T_c} \sim L^{\frac{\gamma}{\nu}}$, which are approximately satisfied in the vicinity of the critical temperatures. The vertical colored lines are critical temperatures and the black horizontal lines correspond to the values of the exponents for the 2D Ising universality class ($\eta = 1/4$ and $\gamma/\nu = 7/4$).

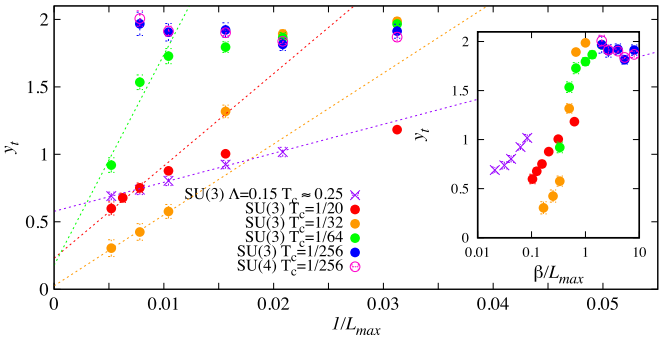

FIG. 7. (Color online) System-size dependence of y_t estimated from B_R. All y_t values were evaluated from the Bayesian scaling analysis for several data sets labeled $L_{\max}$ (see text). The extrapolated values are expected to be those in the thermodynamic limit. The dotted line is a guide for the eye. The inset is the same result plotted as a function of $\beta/L_{\max}$. Note that $k_B = 1$ and $J + Q_2 = 1$.

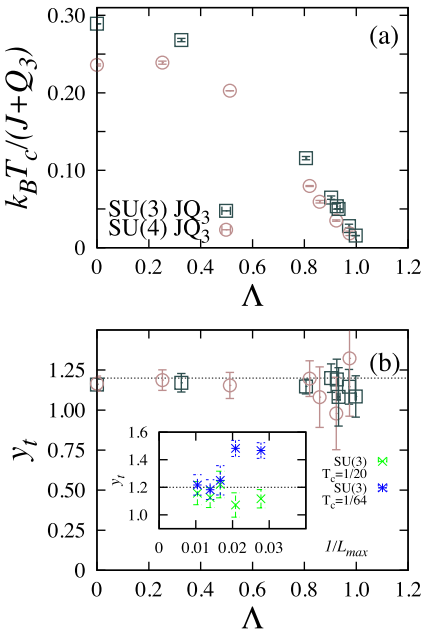

FIG. 8. (Color online) (a) Critical temperature and (b) renormalization group eigenvalue for temperature in the honeycomb-lattice case. y_t is also evaluated from extrapolation to the thermodynamic limit. The inset of panel (b) is the system-size dependence of y_t for the results obtained from the fixed-temperature calculations at $k_BT_c/(J + Q_3) = 1/20$ and $1/64$ (see text). The open squares (circles) are the results for the SU(3) [SU(4)] spins. The black dotted line is the value of the 2D three-state Potts case, $y_t = 6/5$.

the 2D Ising universality class. y_t (ν) itself varies depending on Λ, but the other exponents, such as η and γ/ν, are constant. This behavior is known as the 2D Ising weak universality [19] and is consistent with the results reported in Ref. [16] for the SU(2) JQ_3 model.

To approach the QPT point from the finite-temperature region, we performed these calculations at very low fixed temperatures by varying λ. With limited system size, we observed an apparent increase in y_t. However, as we discuss below, this is due to crossover from the mean-field-type behavior to the true asymptotic behavior and should not be taken as an evidence suggesting a first-order transition. (This is a slightly confusing point since the mean-field value for $y_t = 2$ happens to be equal to the expected value for the first-order transition in two dimensions.) Figure 7 shows the system-size dependence of y_t at $k_BT/(J + Q_2) = 1/20, 1/32, 1/64$, and $1/256$ for the SU(3) case. Each value of y_t is the FSS result of B_R for several data sets labeled $L_{\max}$ that include three different system sizes; for example, $L_{\max} = 48$ includes $L = \{24,32,48\}$, $L_{\max} = 72$ contains $L = \{48,64,72\}$, and so on. At $k_BT/(J + Q_2) = 1/20$, y_t *systematically* decreases as $L_{\max}$ increases and takes the approximate value $y_t \sim 0.23$ in the thermodynamic limit. However, in the lower-temperature region, we observe that y_t exhibits a crossover from the mean-field value; the data for small $L_{\max}$ indicate $y_t \sim 2(= \frac{1}{\nu})$, but y_t decreases suddenly when the system size becomes larger than a characteristic length, L_c. In the case of $k_BT/(J + Q_2) = 1/32$ and $k_BT/(J + Q_2) = 1/64$, we estimated $L_c \sim 72$ and $L_c \sim 192$, respectively. However, when $k_BT_c/(J + Q_2) = 1/256$, we obtained a data with the exponents of the mean-field value in both the SU(3) and the SU(4) case. Therefore, we can obtain the correct values from the data for $L > L_c$ in the FSS analysis, while we estimate the mean-field values from the $L < L_c$ data. This L_c is natively related to the development of the correlation length along the imaginary-time direction, ξ_τ; the thermal criticality can be observed after ξ_τ approximately exceeds the inverse temperature, β. (It is expected that $L_c \sim \xi_\tau \sim a\beta$, where a is an unknown constant.) In the present case, the correlation along the real space direction is well developed for $\xi_\tau < \beta$. Thus, the system can be described by an effective model with long-range interactions. Similar crossover is observed for the critical exponent y_t ($= 1/\nu$) in the 2D Ising models with long-range interactions [28]. In the Ising model, y_t depends on the ratio between the interaction range and system size. When the interacting range is significantly larger than the system size, mean-field-type behavior is observed. From the extrapolated results for y_t, it can be stated that the universality class of the thermal transition for $k_BT_c/(J + Q_2) \geqslant 1/64$ is explained by that of the 2D classical $XY + Z_4$ model and is therefore the weak 2D Ising universality class.

Next, we focus on the criticality of the SU(N) JQ_3 model on the honeycomb lattice. In Fig. 8, we summarize $y_t = \nu^{-1}$ and T_c for the SU(3) and SU(4) JQ_3 models. We find that $y_t = 6/5$ ($\nu = 5/6$) is well satisfied even in the vicinity of the QPT limit of $\Lambda = 1$ and that the size dependence of y_t is quite small for $\Lambda \lesssim 0.95$. This value is consistent with that of the 2D three-state Potts universality. In Fig. 9, we show η and γ/ν that were estimated in the same manner as in the square-lattice case. The 2D three-state Potts universality is also confirmed directly; $\eta = 4/15$ and $\gamma/\nu = 26/15$ are satisfied at the critical temperatures within error bars. The present columnar VBS pattern is characterized by the $\pi/3$ rotational symmetry breaking, reflecting the honeycomb-lattice background. Thus, it is expected that the related classical model with the same universality class is the 2D $XY + Z_3$ model. Since the Z_3 field is strongly relevant in two dimensions, the exponents are not affected by the coupling constants J and Q_3.

The fact that the Z_3 field is relevant may help us discuss the possibility of DCP occurring. If the present honeycomb

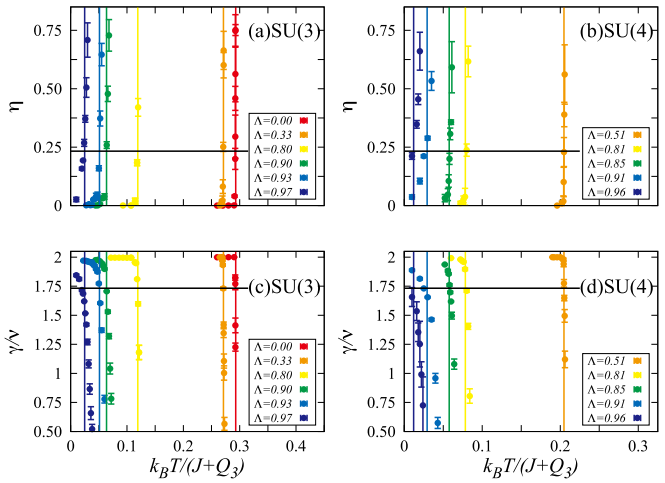

FIG. 9. (Color online) Λ dependence of estimated η and γ/ν for the JQ_3 model on the honeycomb lattice. Panels (a) and (b) [panels (c) and (d)] are η (γ/ν) results for the SU(3) and SU(4) cases, respectively. The vertical colored lines denote critical temperatures and the black horizontal lines are critical exponents for the 2D three-state Potts model, $\eta = 4/15$ and $\gamma/\nu = 26/15$.

JQ_3 model can be well mapped onto the 2D three-state Potts model and the change in the coupling ratio can be regarded as the variation of certain parameters, for example, the transverse field in the conventional 2D Ising model, the criticality in the QPT limit is explained by the 3D three-state Potts model. In that case, the QPT should exhibit a weak first-order transition [18,29–31] and the first-order transition line should extend in the finite-temperature region. The length of the first-order transition line may be finite but is too short to be observed [see Fig. 1 (b)]. This means that the value of ν should change from the 2D three-state Potts value to the trivial value of $\nu = 1/D$ ($D = 2$) via the value at the multicritical fixed point. However, such crossover behavior is not observed when the system approaches the QPT point. We also perform the fixed-temperature calculations for the honeycomb-lattice case. When we vary λ for fixed $k_BT/(J + Q_3) = 1/64$, where the critical point corresponds to $\Lambda \sim 0.99$, the 2D three-state Potts universality is still observed. Figure 10 shows the FSS results for the SU(3) case. We obtain data collapse for $L > 80$ if we set the critical exponents to those of the 2D three-state Potts universality. In the case of the honeycomb-lattice model,

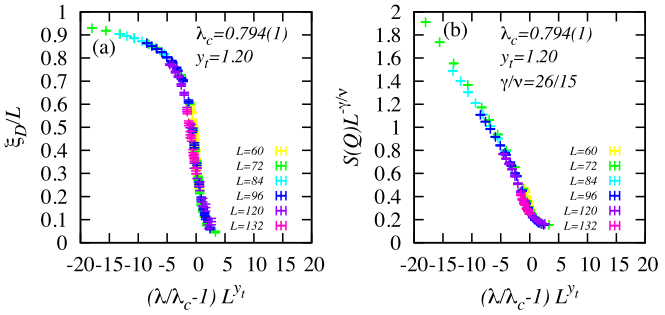

FIG. 10. (Color online) Finite-size scaling analysis for the SU(3) honeycomb-lattice case at $k_BT/(J + Q_3) = 1/64$. (a) Correlation length. (b) Static structure factor.

we expect that the crossover behavior from the mean-field theory exists for $L < 80$, but it is very weak. Therefore, it is difficult to identify the conventional system-size dependence. This result indicates that the development of L_c is relatively suppressed in comparison with the square-lattice case at the same temperature.

The obtained thermal phase diagram for $\Lambda \lesssim 0.99$ supports the possibility of scenario (a) in Fig. 1, because it seems unlikely that ν will approach the trivial value of $1/D$ in both the square-lattice and the honeycomb-lattice cases. If the scenario (b) occurs, the multicritical point should exist at quite a low temperature, i.e., $k_BT/(J + Q_m) < O(10^{-2})$. This is still consistent with our previous discussion of the QPT point [14]; a systematic increase in $\nu_{\rm QPT}$ towards the trivial value is observed for $L > 128$ in the SU(3) square-lattice model. If the dynamical exponent for the DCP is unity, $k_BT/(J + Q_m) < O(10^{-2})$ corresponds to the length scale $L > O(10^2)$. This implies that the correlation length is very large and almost diverging.

IV. SUMMARY

In this paper, we have investigated the thermal transitions of JQ_2 models on the square lattice and JQ_3 models on the honeycomb lattice for SU(3) and SU(4) spins. We have found that the criticality of the SU(N) square-lattice model is well explained by the 2D weak Ising universality class in both the SU(3) and SU(4) cases, which is in agreement with Jin and Sandvik's result [16] for the SU(2) JQ_3 model. The thermal exponent, ν, monotonically increases as the system approaches the QPT limit, and the decrease in ν that should occur if ν eventually reaches its first-order transition value of $1/D$ has not been observed. Thus, the first-order transition appears to be less likely for $k_BT_c/(J + Q_m) > O(10^{-2})$. In the honeycomb-lattice case, reflecting the fact that the Z_3 field is strongly relevant, ν always exhibits the 2D three-state Potts value. From the obtained results, we have discussed possible scenarios for the thermal phase diagram. If the first-order transition occurs, we may observe critical behaviors with strong system-size corrections. However for $k_BT_c/(J + Q_m) > 1/64$, crossover behavior is not observed clearly in our results. To determine the thermal phase diagram (a) or (b) occurring in the present models, the numerical calculations for extremely large system sizes are required, because the drastic development of L_c is expected in the vicinity of the QPT.

ACKNOWLEDGMENTS

We thank T. Okubo for fruitful discussions. This work is supported by the MEXT Grand-in-Aid for Scientific Research (b) (Grant No. 25287097) and Scientific Research (c) (Grant No. 26500392). We are grateful for use of the computational resources of the K computer, which was provided by the RIKEN Advanced Institute for Computational Science through the HPCI Research System project (Projects No. hp120283 and No. hp130081), for some calculations in this study. For use of numerical computation resources, we thank the ISSP Supercomputer Center at University of Tokyo and the Research Center for Nano-micro Structure Science and Engineering at University of Hyogo.

[1] V. L. Ginzburg and L. D. Landau, Zh. Eksp. Teor. Fiz. **20**, 1064 (1950).
[2] K. G. Wilson and J. Kogut, Phys. Rep. **12**, 75 (1974).
[3] T. Senthil, A. Vishwanath, L. Balentz, S. Sachdev, and M. P. A. Fisher, Science **303**, 1490 (2004).
[4] T. Senthil, L. Balents, S. Sachdev, A. Vishwanath, and M. P. A. Fisher, Phys. Rev. B **70**, 144407 (2004).
[5] T. Senthil, L. Balents, S. Sachdev, A. Vishwanath, and M. P. A. Fisher, J. Phys. Soc. Jpn. **74**, 1 (2005).
[6] A. W. Sandvik, Phys. Rev. Lett. **98**, 227202 (2007).
[7] R. G. Melko and R. K. Kaul, Phys. Rev. Lett. **100**, 017203 (2008).
[8] A. B. Kuklov, M. Matsumoto, N. V. Prokof'ev, B. V. Svistunov, and M. Troyer, Phys. Rev. Lett. **101**, 050405 (2008).
[9] J. Lou, A. W. Sandvik, and N. Kawashima, Phys. Rev. B **80**, 180414 (2009).
[10] A. W. Sandvik, Phys. Rev. Lett. **104**, 177201 (2010).
[11] R. K. Kaul and A. W. Sandvik, Phys. Rev. Lett. **108**, 137201 (2012).
[12] K. Chen, Y. Huang, Y. Deng, A. B. Kuklov, N. V. Prokof'ev, and B. V. Svistunov, Phys. Rev. Lett. **110**, 185701 (2013).
[13] S. Pujari, K. Damle, and F. Alet, Phys. Rev. Lett. **111**, 087203 (2013).
[14] K. Harada, T. Suzuki, T. Okubo, H. Matsuo, J. Lou, H. Watanabe, S. Todo, and N. Kawashima, Phys. Rev. B **88**, 220408(R) (2013).
[15] M. Tsukamoto, K. Harada, and N. Kawashima, J. Phys.: Conf. Ser. **150**, 042218 (2009).
[16] S. Jin and A. W. Sandvik, Phys. Rev. B **87**, 180404(R) (2013).
[17] J. Ashkin and E. Teller, Phys. Rev. **64**, 178 (1943).
[18] F. Y. Wu, Rev. Mod. Phys. **54**, 235 (1982).
[19] M. Suzuki, Prog. Theor. Phys. **51**, 1992 (1974).
[20] J. V. José, L. P. Kadanoff, S. Kirkpatrick, and D. R. Nelson, Phys. Rev. B **16**, 1217 (1977).
[21] E. Rastelli, S. Regina, and A. Tassi, Phys. Rev. B **69**, 174407 (2004).
[22] E. Rastelli, S. Regina, and A. Tassi, Phys. Rev. B **70**, 174447 (2004).
[23] R. J. Baxter, *Exactly Solved Models in Statistical Mechanics* (Academic Press, London, 1982).
[24] S. Sachdev and R. A. Jalabert, Mod. Phys. Lett. B **04**, 1043 (1990).
[25] S. Todo, H. Matsuo, and H. Shitara (unpublished).
[26] B. Bauer, L. D. Carr, H. G. Evertz, A. Feiguin, J. Freire, S. Fuchs, L. Gamper, J. Gukelberger, E. Gull, S. Guertler *et al.*, J. Stat. Mech. (2011) P05001.
[27] K. Harada, Phys. Rev. E **84**, 056704 (2011).
[28] E. Luijten, H. W. J. Blöte, and K. Binder, Phys. Rev. E **56**, 6540 (1997).
[29] F. Y. Wu, Rev. Mod. Phys. **55**, 315(E) (1983).
[30] H. W. J. Blöte and R. H. Swendsen, Phys. Rev. Lett. **43**, 799 (1979).
[31] W. Janke and P. Villanova, Nucl. Phys. B **489**, 679 (1997).